14

Spin Connection Resonance in the Faraday Disk Generator

by

Myron W. Evans,
Alpha Institute for Advanced Study, Civil List Scientist.
(emyrone@aol.com and www.aias.us)

and

F. Amador and Horst Eckardt,
Alpha Institute for Advanced Studies (AIAS).

Abstract

Using Einstein Cartan Evans (ECE) unified field theory the conditions are deduced under which a Faraday disk generator may be used to demonstrate a resonant peak of power due to the spin connection used in ECE theory (spin connection resonance or SCR). The analytical analysis is supported by a Faraday disk design with variable spin speeds which has recently demonstrated the existence of SCR experimentally. Three principal types of resonances have been identified.

Keywords: ECE theory, spin connection resonance, Faraday disk generator.

14.1 Introduction

During the course of development [1–10] of ECE theory the phenomenon of spin connection resonance (SCR) has been developed (for example papers 63 and 94 of the ECE series on www.aias.us) and shown to be important in the acquisition of electric power from space-time through the Cartan torsion. This source of electric power is well known experimentally and was demonstrated for example by Tesla [11] in several devices. Other groups have

observed such effects [1–10] for over a hundred years, but as in the case of the Faraday disk generator [12] the standard Maxwell Heaviside (MH) theory does not have an explanation for them. Therefore there has been a tendency to under-implement these potentially important devices despite their obvious importance for the generation of electric power. In papers 43 and 44 of the ECE series a straightforward explanation for the Faraday disk generator was given in terms of the spinning of space-time and in Section 14.2 this explanation is adapted to demonstrate analytically the possibility in the Faraday disk generator of spin connection resonance induced by varying the speed of the spinning disk. Further details and numerical evaluations are given in Section 14.3. In Sections 14.4 and 14.5 such a device is described experimentally and suggestion is made for the improved control and engineering of devices that take electric power from space-time using the Faraday disk design.

14.2 Analytical Theory

The theory of the Faraday disk was first developed with ECE theory in papers 43 and 44. They were based on the fundamental idea of ECE theory:

$$F = A^{(0)}T \tag{14.1}$$

in short-hand index-less notation [1–10]. Here F denotes the electromagnetic field form and T the Cartan torsion form [13, 14]. The quantity $cA^{(0)}$ is a fundamental voltage [1–10]. In the Faraday disk the torsion T is set up by mechanical rotation. So the basic equations of the generator are:

$$F = A^{(0)}T(\text{mechanical}) = d \wedge A + \omega \wedge A \tag{14.2}$$

where $\wedge$ denotes wedge product and $d\wedge$ denotes exterior derivative. Here A is the potential form of ECE theory [1–10] and ω is its spin connection form [1–10, 13, 14]. The field equations of the system are based on the Bianchi identity as developed by Cartan and are:

$$d \wedge F + \omega \wedge F = R \wedge A, \tag{14.3}$$

$$d \wedge \tilde{F} + \omega \wedge \tilde{F} = \tilde{R} \wedge A. \tag{14.4}$$

The second equation is the Hodge dual of the Bianchi identity and was developed during the course of development of ECE theory. The field equations can be reduced [1–10] to vector notation as used in standard electrical engineering. They then become the following set of six equations for all practical purposes in the laboratory.

$$\boldsymbol{\nabla} \cdot \mathbf{B} = 0 \tag{14.5}$$

$$\boldsymbol{\nabla} \times \mathbf{E} + \frac{\partial \mathbf{B}}{\partial t} = 0 \tag{14.6}$$

$$\boldsymbol{\nabla} \cdot \mathbf{E} = \frac{\rho}{\epsilon_0} \tag{14.7}$$

$$\boldsymbol{\nabla} \times \mathbf{B} - \frac{1}{c^2} \frac{\partial \mathbf{E}}{\partial t} = \mu_0 \mathbf{J} \tag{14.8}$$

$$\mathbf{B} = \boldsymbol{\nabla} \times \mathbf{A} - \boldsymbol{\omega} \times \mathbf{A} \tag{14.9}$$

$$\mathbf{E} = -\boldsymbol{\nabla}\phi - \frac{\partial \mathbf{A}}{\partial t} + \phi \boldsymbol{\omega} - \omega \mathbf{A}. \tag{14.10}$$

The first four are the Gauss law, the Faraday law of induction, the Coulomb law and the Ampère Maxwell law, the fifth and sixth are the equations expressing fields in terms of the potentials and spin connection scalar and vector. In these vector equations, expressed in S.I. units, $\mathbf{B}$ is the magnetic flux density, $\mathbf{E}$ is the electric field strength, ρ is the charge density, ϵ_0 is the vacuum permittivity, $\mathbf{J}$ is the current density, $\mathbf{A}$ is the vector potential, ω is the scalar connection, ϕ is the scalar potential and $\boldsymbol{\omega}$ is the vector connection. Details of this derivation are given in the ECE series of papers and books (www.aias.us), notably in review paper 100.

The Bianchi identity (14.3) gives the homogeneous field equation in tensor notation, and the Hodge dual identity (14.4) gives the inhomogeneous field equation in tensor notation. The tensor equations are then written in the base manifold, which is a four dimensional space-time with torsion and curvature. The latter is expressed in the original field equations through the curvature form R in index-less notation, the link between geometry and the electromagnetic field being expressed by the basic relation (14.2). The classical field equations of electrodynamics therefore become field equations of general relativity, not field equations of special relativity, in which both torsion and curvature are absent, and in which the space-time is a Minkowski space-time. The MH field theory, in which the electromagnetic field is a nineteenth century concept defined on a Minkowski frame of reference, is one of special relativity. In ECE theory the electromagnetic field is the space-time geometry itself within a factor $A^{(0)}$, where $cA^{(0)}$ is a primordial voltage. Finally the two tensor equations in the base manifold are developed as four vector equations, and the tensor relation between field and potential developed into two further vector equations.

In paper 44 a complex circular basis [1–10] was used to define a rotating potential set up by mechanically rotating the Faraday disk at an angular frequency Ω in radians per second:

$$\mathbf{A}^{(1)} = \frac{A^{(0)}}{\sqrt{2}} (\mathbf{i} - i\mathbf{j}) e^{i\Omega t}. \tag{14.11}$$

Its complex conjugate is denoted:

$$\mathbf{A}^{(2)} = \frac{A^{(0)}}{\sqrt{2}} (\mathbf{i} + i\mathbf{j})\, e^{-i\Omega t}. \tag{14.12}$$

This is the key concept of the ECE explanation of the Faraday disk generator. The real parts of $\mathbf{A}^{(1)}$ and $\mathbf{A}^{(2)}$ are the same and can be worked out with de Moivre's Theorem:

$$e^{i\Omega t} = \cos \Omega t + i \sin \Omega t. \tag{14.13}$$

The ECE concept is based on:

$$A = A^{(0)} q \tag{14.14}$$

where q is the Cartan tetrad [1–10]. The tetrad relevant to the Faraday disk is:

$$\mathbf{q}^{(1)} = \mathbf{q}^{(2)*} = \frac{1}{\sqrt{2}} (\mathbf{i} - i\mathbf{j})\, e^{i\Omega t}. \tag{14.15}$$

This concept is one of rotational general relativity, whereas the Maxwell Heaviside (MH) theory is one of special relativity in a flat or Minkowski space-time. It is well known that MH is unable to explain the Faraday disk generator, whereas ECE explains it straightforwardly. It is clear therefore that electrodynamics is part of ECE theory, a generally covariant unified field theory (www.aias.us). Classical and quantum electrodynamics have been extensively developed within ECE theory, and unified with other fundamental fields, notably gravitation.

In the Faraday disk the mechanical spin sets up a rotational tetrad, which is a rotation of space-time ITSELF. In paper 44 a special case of Eq. (14.10) was used:

$$\mathbf{E} = -\frac{\partial \mathbf{A}}{\partial t} - \omega \mathbf{A} \tag{14.16}$$

in which ϕ was assumed to be zero and where $\mathbf{A}$ is generated by the magnet of the Faraday disk generator, essentially as used by Faraday and reported in his diary on Dec 26th 1831. The scalar spin connection in paper 44 was assumed to be proportional to Ω, so the electric field strength is:

$$\mathbf{E}^{(2)} = \mathbf{E}^{(1)*} = -\left(\frac{\partial}{\partial t} + i\Omega\right) \mathbf{A}^{(2)}. \tag{14.17}$$

The real part of this expression is worked out with Eq. (14.13) and is:

$$\mathbf{E} = \frac{2}{\sqrt{2}} A^{(0)} \Omega \left(\mathbf{i} \sin \Omega t - \mathbf{j} \cos \Omega t \right). \tag{14.18}$$

This electric field strength (in volts per meter) spins around the rim of the rotating disk. As observed experimentally it is proportional to the product of $A^{(0)}$ and Ω. An electromotive force is set up between the center of the disk and its rim, as first observed by Faraday, and this emf is measured by a voltmeter at rest with respect to the spinning disk.

Recently [15] there have been reports of a Faraday disk generator exhibiting a powerful resonance effect hitherto unknown. The onset of this surge of electric power occurs when the angular frequency of the spinning disk is time dependent. At a sharply defined Ω the apparatus was observed to disintegrate (explode). There is no explanation for this in standard electrical engineering, which is based on the MH theory. In ECE theory it can be explained by spin connection resonance provided that the rate of spin of the disk is time dependent, i.e. its RPM increases so that:

$$\frac{\partial \Omega}{\partial t} \neq 0. \tag{14.19}$$

Use Eq. (14.8) with

$$\boldsymbol{\nabla} \times \mathbf{B} = \mathbf{0} \tag{14.20}$$

because in the Faraday disk generator:

$$\mathbf{B} = B^{(0)} \mathbf{k}. \tag{14.21}$$

Therefore

$$\frac{\partial \mathbf{E}}{\partial t} = -\epsilon_0 \mathbf{J} \tag{14.22}$$

where:

$$\mathbf{E} = \frac{2}{\sqrt{2}} A^{(0)} \Omega \left(\mathbf{i} \sin \Omega t - \mathbf{j} \cos \Omega t \right). \tag{14.23}$$

and in complex circular notation the electric field strength is:

$$\mathbf{E}^{(2)} = -\frac{\partial \mathbf{A}^{(2)}}{\partial t} - i\Omega \mathbf{A}^{(2)}. \tag{14.24}$$

Differentiating this equation with respect to time:

$$\frac{\partial \mathbf{E}^{(2)}}{\partial t} = -\frac{\partial^2 \mathbf{A}^{(2)}}{\partial t^2} - i\Omega \frac{\partial \mathbf{A}^{(2)}}{\partial t} - i\frac{\partial \Omega}{\partial t}\mathbf{A}^{(2)} = -\frac{\mathbf{J}}{\epsilon_0}, \tag{14.25}$$

so using Eq. (14.24) the equation for the potential is:

$$\frac{\partial^2 \mathbf{A}^{(2)}}{\partial t^2} + i\Omega \frac{\partial \mathbf{A}^{(2)}}{\partial t} + i\frac{\partial \Omega}{\partial t}\mathbf{A}^{(2)} = \frac{\mathbf{J}}{\epsilon_0}. \tag{14.26}$$

This is an Euler Bernoulli resonance equation [1–10, 16] under the condition:

$$\frac{\partial \Omega}{\partial t} \neq 0 \tag{14.27}$$

i.e. that the RPM of the spinning disk increases. Thus:

$$\frac{\partial^2 \mathbf{A}^{(2)}}{\partial t^2} + i\frac{\partial \left(\Omega \mathbf{A}^{(2)}\right)}{\partial t} = \frac{\mathbf{J}}{\epsilon_0}. \tag{14.28}$$

This is an undamped resonator equation if J is designed experimentally to be periodic, for example:

$$\mathbf{J}^{(2)} = J^{(0)} \cos(\Omega_0 t)\, \mathbf{e}^{(2)}. \tag{14.29}$$

Finally if the engineering design is such that:

$$\frac{\partial \Omega}{\partial t} >> \Omega \tag{14.30}$$

we obtain the equation:

$$\frac{\partial^2 \mathbf{A}^{(2)}}{\partial t^2} + i\frac{\partial \Omega}{\partial t}\mathbf{A}^{(2)} = J^{(0)} \cos(\Omega_0 t)\, \mathbf{e}^{(2)}. \tag{14.31}$$

At resonance [1–10, 16]:

$$\mathbf{A}^{(2)} \to \infty. \tag{14.32}$$

The observed explosion of the Faraday disk generator [15] may be explained in this way, i.e. the design must be a rapidly varying Ω and a periodic current density coming from the emf set up between the center and rim of the rotating disk.

14.3 Numerical Results

The resonance equation (14.26) has to be solved nuerically. First we rewrite the equation to two equations for the real and imaginary part of $\mathbf{A}^{(2)}$, denoted by A_r and A_i (considering only the time dependence):

$$\frac{d^2 A_r}{dt^2} - A_i \left(\frac{d\Omega}{dt}\right) - \left(\frac{dA_i}{dt}\right)\Omega = \frac{J}{\epsilon_0}, \tag{14.33}$$

$$\frac{d^2 A_i}{dt^2} + A_r \left(\frac{d\Omega}{d\,t}\right) + \left(\frac{dA_r}{dt}\right)\Omega = 0. \tag{14.34}$$

In case of vanishing Ω these equations pass into

$$\frac{d^2 A_r}{dt^2} = \frac{J}{\epsilon_0}, \tag{14.35}$$

$$\frac{d^2 A_i}{dt^2} = 0. \tag{14.36}$$

These simple equations then have the general solutions

$$A_r = \frac{J}{2\epsilon_0} t^2 + k_1 t + k_2, \tag{14.37}$$

$$A_i = k_3 t + k_4. \tag{14.38}$$

These are growing solutions in t, even if the constants k_1 and k_2 are chosen as zero. Therefore the real part of the electric Field (see Eq. (14.24))

$$E_r = Re\left(-\frac{\partial A}{\partial t} - i\Omega A\right) = A_i\,\Omega - \frac{dA_r}{dt}. \tag{14.39}$$

will grow linearly by the mechanical rotation. The effect of Ω will be to overlay an oscillatory structure to the simple solutions (14.37), (14.38).

For the numerical solution of Eqs. (14.33, 14.34) we define

$$\Omega = \alpha_0 \cos\,\omega_0 t, \tag{14.40}$$

$$J = J_0 \cos\,\omega_J\, t. \tag{14.41}$$

To make the simulations more realistic we have added a conductivity term according to Ohm's law:

$$\mathbf{J}_{cond} = \sigma\,\mathbf{E} \tag{14.42}$$

with a suitable conductivity value σ. Replacing $\mathbf{J}$ by $\mathbf{J} + \mathbf{J}_{cond}$ in Eq. (14.26) and selecting the real and imaginariy part again leads to

$$\frac{d^2 A_r}{dt^2} - A_i \left(\frac{d\Omega}{dt}\right) - \left(\frac{dA_i}{dt}\right) \Omega = \frac{J}{\epsilon_0} + \frac{\sigma}{\epsilon_0} \left(A_i\, \Omega - \frac{dA_r}{dt}\right), \tag{14.43}$$

$$\frac{d^2 A_i}{dt^2} + A_r \left(\frac{d\Omega}{dt}\right) + \left(\frac{dA_r}{dt}\right) \Omega = -\frac{\sigma}{\epsilon_0} \left(A_r\, \Omega + \frac{dA_i}{dt}\right). \tag{14.44}$$

Equations (14.33,14.34) have been solved numerically. The results for a moderate amplitude of mechanical rotation are shown in Figs. (14.1)–(14.3). In Fig. (14.1) the real and imaginary part of the vector potential are graphed. The real part grows quadratically as predicted by Eq. (14.37), with a superimposed oscillatory structure by the mechanical rotation Ω. The imaginary part of the potential is purely oscillatory as are both time derivatives (Fig. (14.2)). The most relevant quantity is the electric field, Eq. (14.39), which describes the induction effect due to rotation. As can be seen from Fig. (14.3), The real part of E grows linearly, despite of the oscillating potentials, only in right-most part there is a very low undulation.

For a modified parameter set we chose similar values of mechanical and current frequency, leading to a heterodyne effect in the time behaviour of the potential (Figs. (14.4), (14.5)). The electrical field (Fig. (14.6)) is oscillatory now. The imaginary part is practically zero because the model does not contain any damping or energy dissipation terms.

There should be a resonance behaviour according to section 14.1. In Fig. (14.7) the maximum electric field value within $60s$ simulated time has been

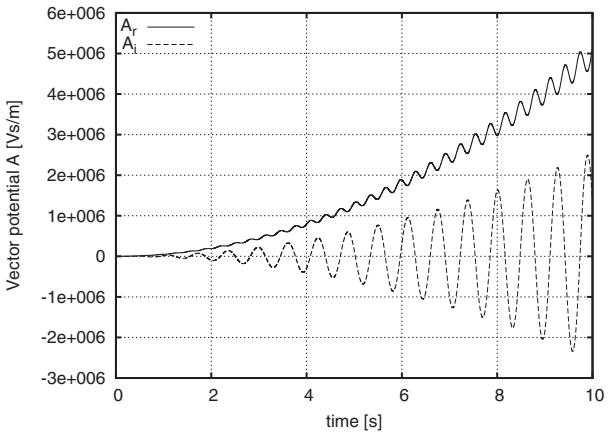

Fig. 14.1. Vector potental for $\alpha_0 = 5$, $\omega_0 = 10$, $\omega_J = 0$.

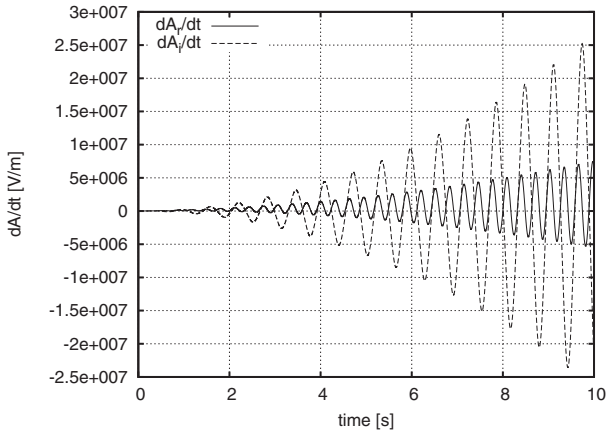

Fig. 14.2. Derivative of Vector potental for $\alpha_0 = 5$, $\omega_0 = 10$, $\omega_J = 0$.

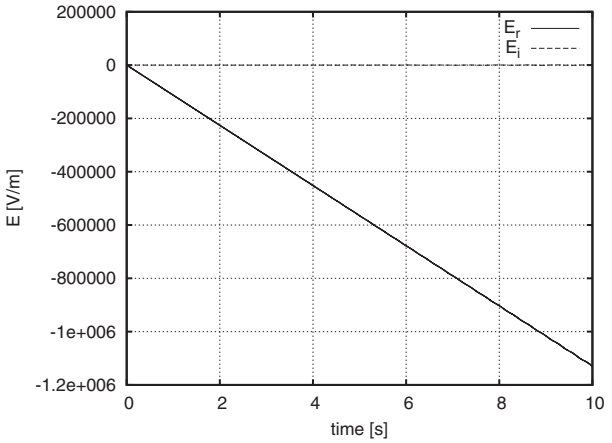

Fig. 14.3. Electric field for $\alpha_0 = 5$, $\omega_0 = 10$, $\omega_J = 0$.

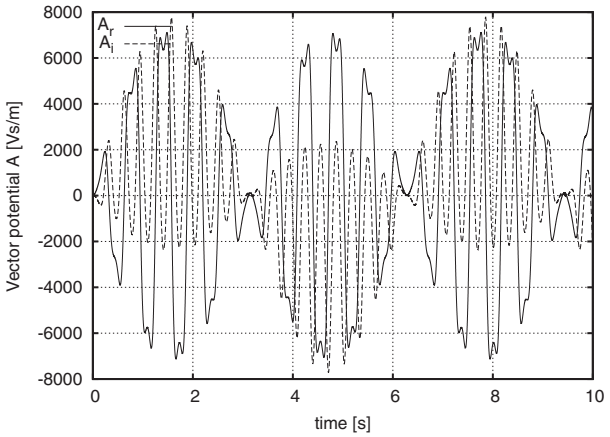

Fig. 14.4. Vector potental for $\alpha_0 = 20$, $\omega_0 = 10$, $\omega_J = 9$.

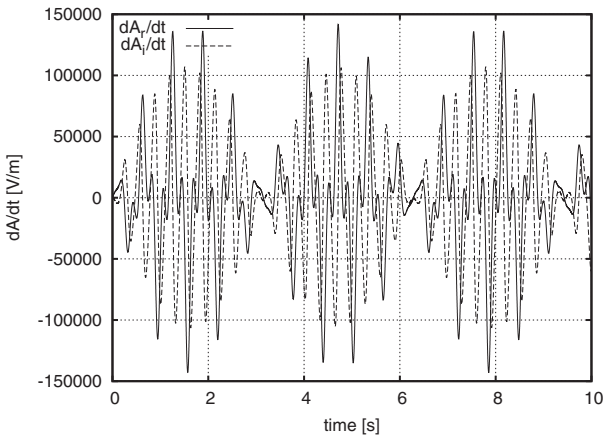

Fig. 14.5. Derivative of Vector potental for $\alpha_0 = 20$, $\omega_0 = 10$, $\omega_J = 9$.

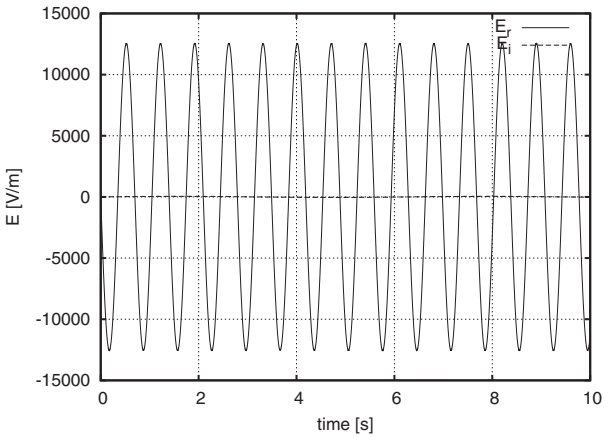

Fig. 14.6. Electric field for $\alpha_0 = 20$, $\omega_0 = 10$, $\omega_J = 9$.

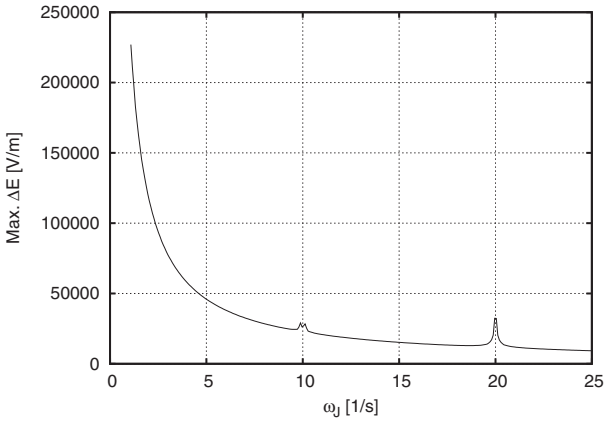

Fig. 14.7. Resonance curve of E field for variable current frequency ω_J.

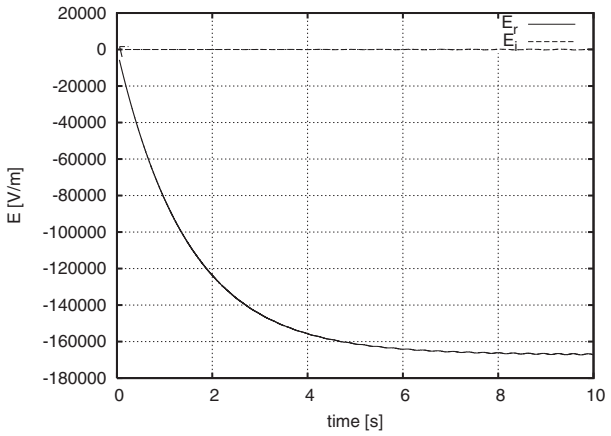

Fig. 14.8. Electric field for $\alpha_0 = 5$, $\omega_0 = 10$, $\omega_J = 0$ with conductivity term.

plotted in dependence of the current frequency ω_J. There are minor maxima for ω_J values of 10/s and 20/s which correspond to the given rotational frequency of $\omega_0 = 10/s$. Most significant is the increase of the maximum amplitude for $\omega_J \to 0$. This means that a direct current gives the highest E field value.

From electrical engineering it is known that the feedback of the electric field to a current can be modeled by Ohm's law, see Eq. (14.42). The resulting Eqs. (14.43, 14.44) therefore lead to a reduction in current. We have repeated the calculation for Fig. (14.3) with a conductivity term. The result (Fig. (14.8)) shows that there is a limit of the E field strength, making the result more realistic.

14.4 Dynamics of the Homopolar Generator

As described in ECE [1–10], torsion in space-time is electromagnetism. It has further been proposed that Spin Connection Resonance (SCR) is also a critical part of ECE. The connecting evidence between both concepts is present when a varying $d\mathbf{\Omega}/dt$ is applied to a Faraday disk (Homopolar Generator). Moreover, it will be shown that the varying spin connection (identified with $d\mathbf{\Omega}/dt \neq 0$) produces additional accelerations to electrons hereto assumed to be ignored under random collisions and generalized to drift velocity.

The accelerative state of a rotating reference frame is analyzed to the application of moving electrons. As shown in a standard mathematical dictionary of equations [17], a body in acceleration with a rotating reference frame experiences the rotational operator

$$\mathbf{R} \equiv \left(\frac{d}{dt}\right)_{body} + \boldsymbol{\Omega} \times . \tag{14.45}$$

The velocity in the rotating frame of space is

$$\mathbf{v}_{space} = \mathbf{R}\mathbf{r} = \frac{d\mathbf{r}}{dt} + \boldsymbol{\Omega} \times \mathbf{r} \tag{14.46}$$

and the equation expanded to acceleration in space is

$$\mathbf{a}_{space} = \mathbf{R}^2\mathbf{r} = \left(\frac{d}{dt} + \boldsymbol{\Omega}\times\right)^2 \mathbf{r} \tag{14.47}$$

where $\mathbf{r}$ is the coordinate vector in the rotating system. Eq. (14.47) gives a simplified result of

$$\begin{aligned}
\mathbf{a}_{space} &= \left(\frac{d}{dt} + \boldsymbol{\Omega}\times\right)\left(\frac{d\mathbf{r}}{dt} + \boldsymbol{\Omega} \times \mathbf{r}\right) \\
&= \frac{d^2\mathbf{r}}{dt^2} + \frac{d}{dt}\left(\boldsymbol{\Omega} \times \mathbf{r}\right) + \boldsymbol{\Omega} \times \frac{d\mathbf{r}}{dt} + \boldsymbol{\Omega} \times \left(\boldsymbol{\Omega} \times \mathbf{r}\right) \\
&= \frac{d^2\mathbf{r}}{dt^2} + \boldsymbol{\Omega} \times \frac{d\mathbf{r}}{dt} + \frac{d\boldsymbol{\Omega}}{dt} \times \mathbf{r} + \boldsymbol{\Omega} \times \frac{d\mathbf{r}}{dt} + \boldsymbol{\Omega} \times \left(\boldsymbol{\Omega} \times \mathbf{r}\right).
\end{aligned} \tag{14.48}$$

When grouping for Velocity and Angular Velocity,

$$\mathbf{v} \equiv \frac{d\mathbf{r}}{dt}, \tag{14.49}$$

$$\boldsymbol{\alpha} \equiv \frac{d\boldsymbol{\Omega}}{dt}, \tag{14.50}$$

we get

$$\mathbf{a}_{space} = \frac{d^2\mathbf{r}}{dt^2} + 2\,\boldsymbol{\Omega} \times \mathbf{v} + \boldsymbol{\Omega} \times \left(\boldsymbol{\Omega} \times \mathbf{r}\right) + \boldsymbol{\alpha} \times \mathbf{r}. \tag{14.51}$$

As a result, we get four terms

$$\mathbf{a}_{body} = \frac{d^2\mathbf{r}}{dt^2}, \tag{14.52}$$

$$\mathbf{a}_{coriolis} = 2\,\boldsymbol{\Omega} \times \mathbf{v}, \tag{14.53}$$

$$\mathbf{a}_{centrifugal} = \boldsymbol{\Omega} \times (\boldsymbol{\Omega} \times \mathbf{r}) \,, \tag{14.54}$$

$$\mathbf{a}_{angular} = \boldsymbol{\alpha} \times \mathbf{r} \tag{14.55}$$

for all accelerative states for the electron particle. The final acceleration of a body in space is summarized as follows:

$$\mathbf{a}_{space} = \mathbf{a}_{body} + \mathbf{a}_{coriolis} + \mathbf{a}_{centrifugal} + \mathbf{a}_{angular} \tag{14.56}$$

where

1. conventional analysis normally ignores the $d\boldsymbol{\Omega}/dt$ when the assumption of an uniformly rotating frame of reference is given,
2. Coriolis acceleration is assumed to vanish in the background through random collisions within either gas, liquids, or solids, and
3. does not link any of these ignored variables to resonance.

Furthermore, the Lozenz Force Law equation in the coordinates $\mathbf{r}'$ of the rest system is

$$\mathbf{F_L}' = q(\mathbf{E}' + \mathbf{v}' \times \mathbf{B}'). \tag{14.57}$$

We have to transform this equation to the rotating system according to Eq. (14.46):

$$\mathbf{F_L} = q \left(\mathbf{E} + \mathbf{v} \times \mathbf{B} + (\boldsymbol{\Omega} \times \mathbf{r}) \times \mathbf{B} \right). \tag{14.58}$$

To re-study the Homopolar Generator in the context of ECE, we use the Newtonian limit and obtain the equation of motion

$$m\mathbf{a}_{space} = \mathbf{F_L} \tag{14.59}$$

which can be rewritten with aid of Eq. (14.56) to

$$m\mathbf{a}_{body} = \mathbf{F_L} - m \left(\mathbf{a}_{coriolis} + \mathbf{a}_{centrifugal} + \mathbf{a}_{angular} \right). \tag{14.60}$$

With substitution of Eqs. (14.52–14.55) and (14.58) follows

$$\frac{d^2\mathbf{r}}{dt^2} = \frac{q}{m} \left(\mathbf{E} + \mathbf{v} \times \mathbf{B} + (\boldsymbol{\Omega} \times \mathbf{r}) \times \mathbf{B} \right) - 2\,\boldsymbol{\Omega} \times \mathbf{v} - \boldsymbol{\Omega} \times (\boldsymbol{\Omega} \times \mathbf{r}) - \boldsymbol{\alpha} \times \mathbf{r}. \tag{14.61}$$

We assume that $\mathbf{\Omega}$ and $\mathbf{B}$ point into the direction of the z coordinate,

$$\mathbf{\Omega} = \begin{pmatrix} 0 \\ 0 \\ \Omega \end{pmatrix}, \tag{14.62}$$

$$\mathbf{B} = \begin{pmatrix} 0 \\ 0 \\ B \end{pmatrix}, \tag{14.63}$$

and E is oscillating in radial direction,

$$\mathbf{E} = E_0 \cos(\omega_J t)\, \widehat{\mathbf{r}} = E_0 \cos(\omega_J t)\, \frac{\mathbf{r}}{r}. \tag{14.64}$$

Then we obtain for the single terms in Eq. (14.61)

$$\begin{aligned} \mathbf{v} \times \mathbf{B} &= \begin{pmatrix} v_2 B \\ -v_1 B \\ 0 \end{pmatrix}, \quad \mathbf{\Omega} \times \mathbf{v} = \begin{pmatrix} -v_2 \Omega \\ v_1 \Omega \\ 0 \end{pmatrix}, \\ \mathbf{\Omega} \times \mathbf{r} &= \begin{pmatrix} -r_2 \Omega \\ r_1 \Omega \\ 0 \end{pmatrix}, \quad \mathbf{\Omega} \times (\mathbf{\Omega} \times \mathbf{r}) = \begin{pmatrix} -r_1 \Omega^2 \\ -r_2 \Omega^2 \\ 0 \end{pmatrix}, \\ (\mathbf{\Omega} \times \mathbf{r}) \times \mathbf{B} &= \begin{pmatrix} r_1 \Omega B \\ r_2 \Omega B \\ 0 \end{pmatrix}, \quad \boldsymbol{\alpha} \times \mathbf{r} = \begin{pmatrix} -r_2 \frac{d\Omega}{dt} \\ r_1 \frac{d\Omega}{dt} \\ 0 \end{pmatrix}. \end{aligned} \tag{14.65}$$

Inserting these terms into Eq. (14.61) shows that the particle moves in the x-y plane exclusively. The two coupled equations of motion in the rotating frame are

$$\frac{d^2 r_1}{dt^2} = \frac{q}{m} \left(E_0 \cos(\omega_J t)\, \frac{r_1}{\sqrt{r_1^2 + r_2^2}} + v_2 B + r_1 \Omega B \right) + 2 v_2 \Omega + r_1 \Omega^2 + r_2 \frac{d\Omega}{dt}, \tag{14.66}$$

$$\frac{d^2 r_2}{dt^2} = \frac{q}{m} \left(E_0 \cos(\omega_J t)\, \frac{r_2}{\sqrt{r_1^2 + r_2^2}} - v_1 B + r_2 \Omega B \right) - 2 v_1 \Omega + r_2 \Omega^2 - r_1 \frac{d\Omega}{dt}. \tag{14.67}$$

This is a model for the dynamics within the Homopolar Generator. As already stated, we cannot expect that electrons move in a solid in such a way, but it may be a hint for certain effects incurred by mechanical rotation. The Eqs. (14.66,14.67) have been solved numerically similar to the previously discussed results. In order to make the single force contributions visible we have solved the equations with omitting particular terms at the right-hand side. First we studied the Coriolis force being present as the only force. The result is shown in Fig. (14.9) for a constant rotation speed Ω. The orbit of a "free" electron is a spiral as is known from classical mechanics. Fig. (14.10) shows the same for an oscillating Ω. In the rotating coordinate system the particle is pushed back and forth as an effect of the variation of Ω. This is superimposed to the spiralling behaviour. The Lorentz force term in action is graphed in Fig. (14.11), for better graphical representation with a factor of $q/m = -1$. It consists of a force in radial direction (from E field) and a circular orbit (from $v \times B$ term). The result is an open rosette orbit. Near to the center there is a sharp edge where direction is changed abruptly. A detailed analysis showed that the velocity in this point is zero, it is like a classical turning point. The electric and magnetic term alone (not shown) give a linear oscillating orbit and a circular orbit.

All these effect computed together lead to a quite chaotic behaviour (Fig. (14.12)). The radius of the orbit is bound due to the Lorentz force term. The maximum radius taken over a certain time interval can be considered as an indicator for a certain resonance behaviour. In our interpretation this means that the charged particle crosses a certain range faster, leading to a higher current. In Fig. (14.13) this criterion is shown in dependence of a variable "driving force" term ω_J. There are indeed certain resonances which depend in a complicated way on the term $q/m \cdot B$.

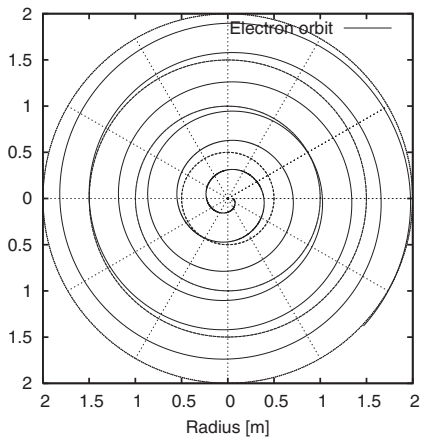

Fig. 14.9. Electron orbit for Coriolis force.

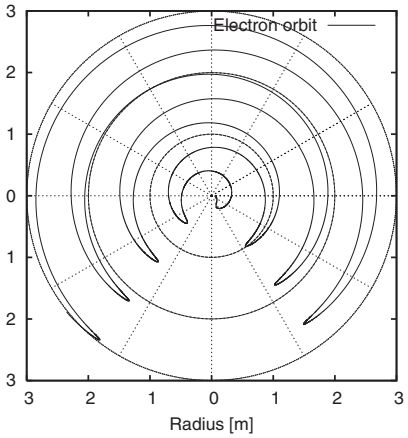

Fig. 14.10. Electron orbit for variable rotation frequency Ω.

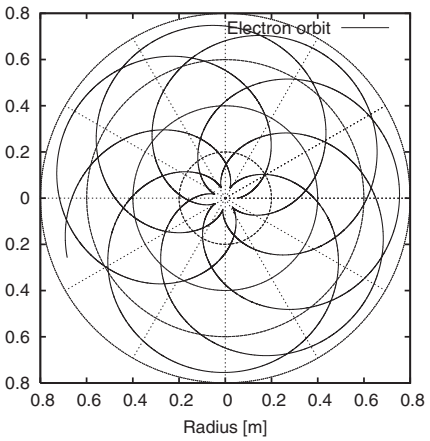

Fig. 14.11. Electron orbit for Lorentz force (electric and magnetic).

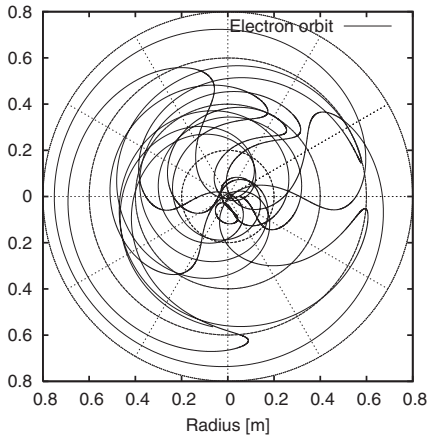

Fig. 14.12. Electron orbit for all force components.

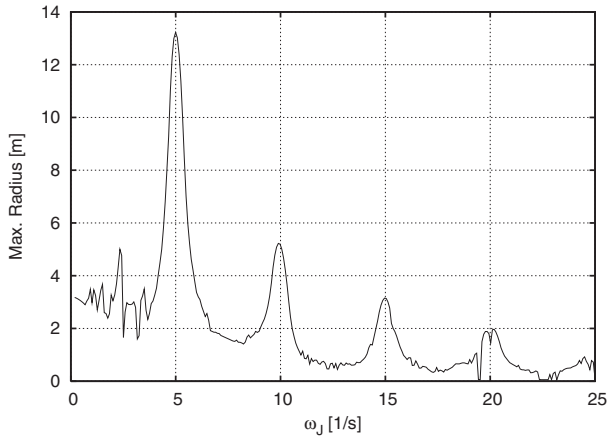

Fig. 14.13. Resonance curve of max. radius for variable current frequency ω_J.

14.5 Discussion of Design

As we have shown in the last section, a varying rotation speed adds sophisticated trajectories to the electron particles within the Homopolar Generator. It is proposed that the relationships (harmonics/standing waves) between Coriolis, centrifugal, and angular accelerations are of key importance; in which, either the geometrical energy being carried by the electrons or the exposed spaces around nucleuses creates additional unrecognized forces.

A detailed prototype of this nature is needed for further study. It's important to notice that additional experiments are needed besides SCR in copper plates; for instance, using aluminum, mercury, carbon nanotubes, superconducting wires, doped semiconducting materials, Stainless Steel, and additional alloys are also good candidates. Moreover, a close study of Weber's Force [18] application to the study of the Homopolar Generator is also needed. A great piece of work concerning classical forces and torque was already done by Guala-Valverde and coworkers (see [25] and references therein).

14.5.1 Magnetic Flux Path Configuration

It is important to mention that a similar path of the accelerated electron just mentioned can be taken by magnetic flux lines by configuring a transformer core away from the usual one pass architecture to many flux path architecture (Fig. (14.14)). A transformer with a coil core design will give flux paths a 1:n relationship amplifying the flux lines through simple geometry. Technically the new architecture would make this the first B(3) Transformer in existence. Engineers using magnets and combination with transformer cores would find this design useful.

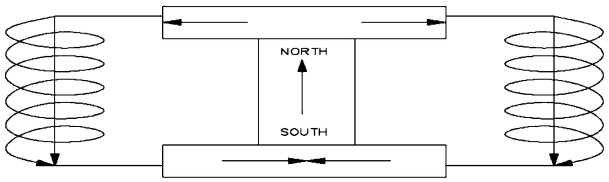

Fig. 14.14. Magnetic flux line amplification by multiple paths.

14.5.2 Proposed Prototype

14.5.2.1 Dynamo Electric Machine

As a result, it is proposed in this document that when SCR & ECE is established, the imposed drift velocities no longer generalize a particles' trajectory and the proposed harmonic/standing waves thru SCR create powerful resonances causing new anomalous results.

The proposed AIAS Homopolar Generator will take on a similar design to Nikola Tesla's work [20], see Fig. (14.15). In his design he proposed a means to extract the energy produced from the spinning disks from the least point on interruptions, the central axis, to both disks. This made his design simple and effective to keep his contacts from experiencing too much wear. Moreover, his design included two disks where a common spin direction produced current from the center-to-periphery of one disk and from the periphery-to-center of the other disk. His arrangements of the magnets made this simple design effective as he tied both disks' periphery with a copper belt band.

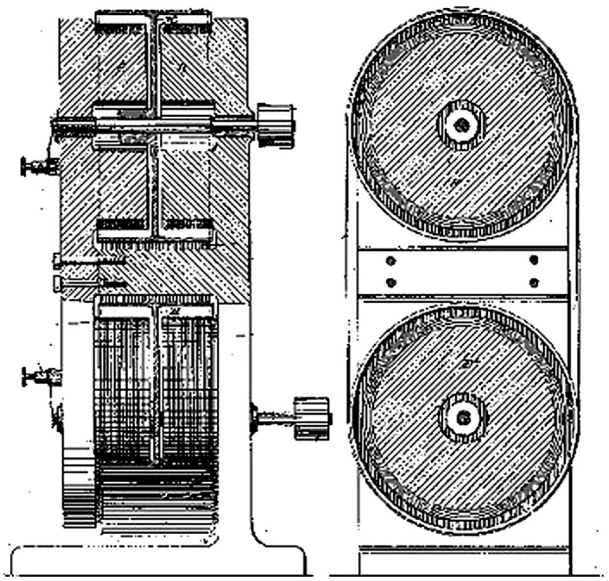

Fig. 14.15. Homopolar generator design of Nikola Tesla.

14.5.2.2 P&ID Detail Control

In our design (Fig. (14.16)) we decouple the outside belts for independent spin control for each Homopolar generator; however, they will have a common coupling point for the amps to flow through between the central axes of both disks. The power will be measured and extracted at the periphery of both disk with contacts going to terminal blocks (V1 and V2) for load connection. The independent spin control of both disks will superimpose two output waves that would give further study to ECE and SCR connection.

The basic AIAS Homopolar Process and Instrumentation Diagram (Fig. (14.16)) shows the general arrangement with Programmable Logic Controllers (PLC) with a Supervisory Control and Data Acquisition (SCADA) package. Standard network protocols (Ethernet and Devicenet) are used for control of

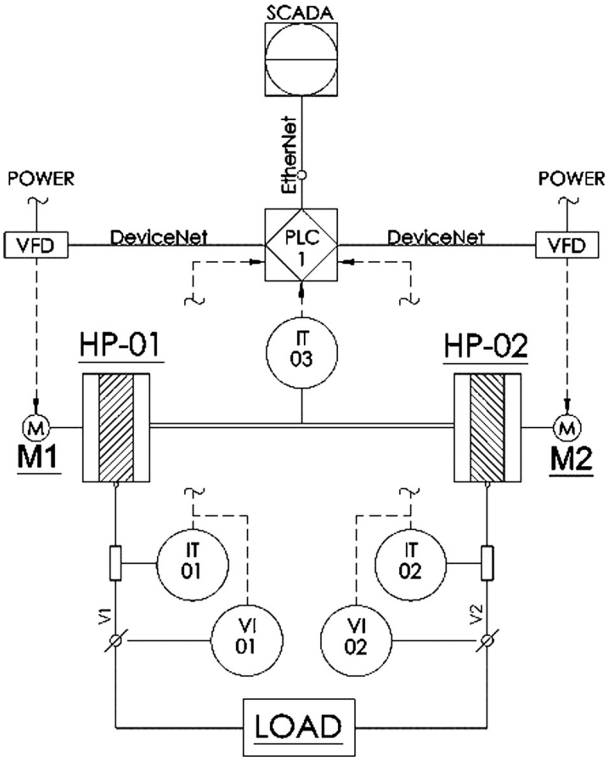

Fig. 14.16. AIAS Homopolar Process & Instrumentation Diagram.

Homopolar generators through variable frequency drives (VFDs) and logging data from instruments and trending of experimental data (SQL Server) are stored in a centralized server. Each instrument shown is for proper data analysis and control of said experiment with Proportional, Integral and Derivative (PID) software.

The final controls design will give both the engineers and scientist the flexibility to either expand or refine the necessary $d\Omega/dt$ control for proper ECE and SCR connections.

14.5.2.3 Circuit Analysis of Current

A circuit analysis of the Homopolar Generator reveals a current source-current output network architecture.

On expansion of this layout it is possible to introduced both positive and negative feedback through an Inductor by adding or subtracting magnetic fields to the static field of the magnets. The inductor would take the arbitrary current produced by the varying current. Since the inductor will be coiled

around the homopolar generator, the end result will be additional input of energy into the system.

As mentioned before, an aligned winding of the inductor to the magnetic fields of the magnet would constitute a positive feedback arrangement. Likewise, if the aligned winding of the inductor is in the opposite direction to the magnetic fields of the magnet then it would constitute a negative feedback. As a result,

$$V(t) = \frac{1}{2}\Omega(t) r^2 B_t \tag{14.68}$$

where

$$B_t = B_{\text{magnet}} + B_{\text{inductor}} \tag{14.69}$$

for positive feedback. Moreover, equation (14.68) becomes

$$V(t) = \frac{1}{2}\Omega(t) r^2 (B_{\text{magnet}} + B_{\text{inductor}}), \tag{14.70}$$

where

$$B_{\text{inductor}} = \mu N \frac{I(t)}{l} \tag{14.71}$$

and

$$V(t) = I(t)\, R. \tag{14.72}$$

Hence, substituting (14.70) and (14.71) into (14.72),

$$I(t)\, R = \frac{1}{2}\left((\Omega(t)\, r^2\, (B_{\text{magnet}} + \mu N \frac{I(t)}{l}) \right) \tag{14.73}$$

or

$$I(t)\left(R - \Omega(t)\, r^2\, \mu N \frac{I(t)}{2l} \right) = \frac{1}{2}\Omega(t)\, r^2\, B_{\text{magnet}}, \tag{14.74}$$

we finally get

$$I(t) = \frac{\Omega(t)\, r^2\, B_{\text{magnet}}}{2\left(R - \Omega(t)\, r^2 \frac{\mu N}{2l} \right)} \tag{14.75}$$

where the known voltages of the system are:

$$V_{\text{homopolar}}(t) = I(t)\, R, \tag{14.76}$$

$$V_{\text{inductor}}(t) = L\frac{dI(t)}{dt} \tag{14.77}$$

so that the total voltage is

$$V_{\text{total}}(t) = I(t)R + L\frac{dI(t)}{dt} \tag{14.78}$$

and total power created by the system is

$$\text{Power}(t) = V_{\text{total}}(t)\, I(t). \tag{14.79}$$

With substitution of (14.78) into (14.79) we get

$$\text{Power}(t) = \left(I(t)R + L\frac{dI(t)}{dt}\right) I(t) \tag{14.80}$$

or

$$\text{Power}(t) = I^2(t)R + L\frac{dI(t)}{dt}I(t). \tag{14.81}$$

For negative feedback, Eq. (14.70) would have a minus before the magnetic field on the inductor indicating that it has been wound in the opposite direction of the magnet's field. Again, this feedback introduces additional standard electrical results which would make the system react much different from the standard Homopolar Generators. We also point out that Tesla did use such inductors on his design to add additional energy into the system.

We conclude with the statement that Eq. (14.75) represent a further type of resonance. The current goes to inifity if the design is chosen in a way that the denominator of this equation tends to zero:

$$R - \Omega(t)\, r^2\, \frac{\mu N}{2l} = 0. \tag{14.82}$$

Assuming the harmonic time behaviour of Eq. (14.40) this gives a resonant current as shown in Fig. (14.17) (in arbitrary units). A time dependent Ω is even not required in this case. Variation of Ω being constant in time leads to the pole-like resonance graphed in Fig. (14.18).

In total we have shown in this paper that in the homopolar generator there are three types of resonances possible: A resonance of potential, a resonance

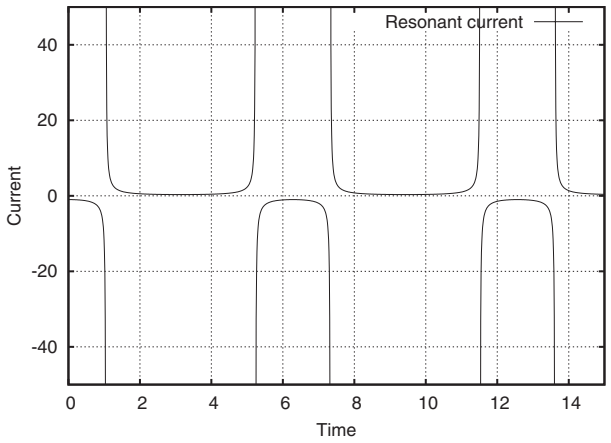

Fig. 14.17. Current resonance according to positive feedback design, periodic $\Omega(t)$.

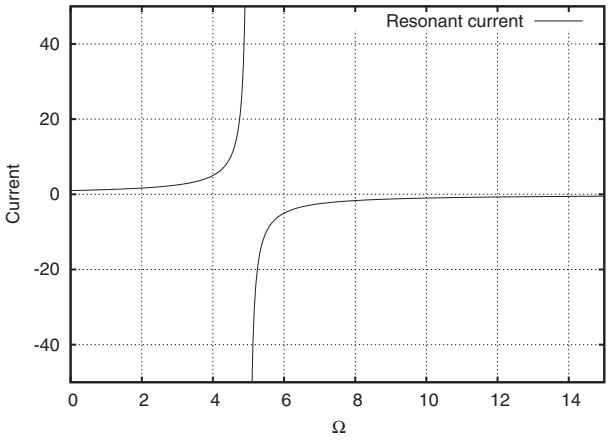

Fig. 14.18. Resonance curve for current resonance, no time-dependent Ω.

due to movement of charge carriers, and a resonance of the current by positive feedback.

Acknowledgments

The British Government is thanked for a Civil List Pension and the staff of AIAS and the Telesio Galilei Association for many interesting discussions.

References

[1] M. W. Evans, "Generally Covariant Unified Field Theory" (Abramis, 2005 onwards), in five volumes to date (see www.aias.us).

[2] L. Felker, "The Evans Equations of Unified Field Theory" (Abramis 2007).

[3] K. Pendergast, "Crystal Spheres" (preprint on www.aias.us, Abramis in prep.).

[4] M. W. Evans and H. Eckardt, Physica B, 400, 175 (2007).

[5] M. W. Evans, Physica B, 403, 517 (2008).

[6] M. W. Evans, Acta Phys. Polonica B, 38, 2211 (2007).

[7] M. W. Evans (ed.), Adv. Chem. Phys., vol. 119 (2001); ibid., M. W. Evans and S. Kielich, vol. 85 (1992, 1993, 1997).

[8] M. W. Evans, Omnia Opera section of www.aias.us, 1992 to present.

[9] M. W. Evans and L. B. Crowell, "Classical and Quantum Electrodynamics and the B(3) Field" (World Scientific, 2001).

[10] M. W. Evans and J.-P. Vigier, "The Enigmatic Photon" (Kluwer, 1994 to 2002), in five volumes.

[11] M. Krause, Director, "All about Tesla", on DVD, Berlin 2007.

[12] T. Valone, "The Homopolar Handbook, A Definite Guide to Faraday Disk and n Machine Technologies"(Integrity Research Institute, 2001, 3rd. Edition).

[13] S. P. Carroll, "Space-time and Geometry, an Introduction to General Relativity" (Addison Wesley, New York, 2004, and 1997 downloadable notes).

[14] R. M. Wald, "General Relativity" (Univ. of Chicago Press, 1984)

[15] Private communication of Walter Thurner to H. Eckardt.

[16] J. B. Marion and S. T. Thornton, "Classical Dynamics" (HBC, New York, 1988, 3rd. Ed.).

[17] E. W. Weisstein, "CRC Concise Encyclopedia of Mathematics" (Chapman & Hall/CRC, 1999)

[18] A. K. T. Assis, "Weber's Electrodynamics" (Kluwer Academic Publishers, 1994)

[19] J. A. Edminister, "Theory and Problems of Electromagnetics" (McGraw Hill Schaum's Outlines Series, 1995, 2nd Edition)

[20] N. Tesla, "My Inventions : The Autobiography of Nikola Tesla", (Barnes & Noble, 1995, reprint)

[21] Programmable Logic Controllers (www.ab.com)

[22] FactoryHMI and FactorySQL SCADA package (www.inductiveautomation.com)
[23] ODVA Devinet protocol (www.odva.org)
[24] PowerFlex Variable Frequency Drives (www.ab.com)
[25] J. Guala-Valverde and R. Achilles, "Ampère: The Avis Phoenix of Electrodynamics", Apeiron, Vol. 15, No. 3, July 2008